Drift Forces on Vacancies and Interstitials in Alloys with Radiation-Induced Segregation

W.G. Wolfer

September 1982

UWFDM-483

J. Nucl. Matls. 00, 0 (1982).

Drift Forces on Vacancies and Interstitials in Alloys with Radiation-Induced Segregation

W.G. Wolfer

Fusion Technology Institute
University of Wisconsin
1500 Engineering Drive
Madison, WI 53706

http://fti.neep.wisc.edu

September 1982

UWFDM-483

J. Nucl. Matls. 00, 0 (1982).

DRIFT FORCES ON VACANCIES AND INTERSTITIALS IN ALLOYS WITH RADIATION-INDUCED SEGREGATION

W.G. Wolfer

Fusion Engineering Program
Nuclear Engineering Department
University of Wisconsin-Madison
Madison, Wisconsin 53706

September 1982

UWFDM-483

Abstract

Radiation-induced segregation in alloys leads to compositional gradients around point defect sinks such as voids and dislocations. These compositional gradients in turn affect the drift forces on both interstitials and vacancies and thereby modify the bias. Linear irreversible thermodynamics is employed to derive the total drift force on interstitials and vacancies in substitutional binary alloys. The obtained results are evaluated for binary Fe-Ni alloys.

It is shown that radiation-induced segregation produces new drift forces which can be of the same order of magnitude as the stress-induced drift force produced by edge dislocations in an alloy with uniform composition. Hence, segregation results in a significant modification of the bias for void nucleation and swelling.

The additional drift forces on interstitials and vacancies are due to the compositional dependence of the formation and migration energies; due to the dependence of the point defect's strain energy on the local elastic properties; due to a coherency strain field caused by lattice parameter variations; and finally due to the Kirkendall force produced by the difference in tracer mobilities.

Estimates of these forces given for Fe-Ni alloys indicate that the Kirkendall force is small compared to the other segregation-induced forces on interstitials. In contrast, the Kirkendall force seems to be the dominant one for vacancies.

1. INTRODUCTION

The segregation of solute elements to point defect sinks has been observed in numerous alloys after irradiation. As reported in the literature, and in particular at two recent symposia [1,2], solute segregation has been found near external surfaces, at grain boundaries, and around voids and dislocation loops. The experimental evidence as well as the general physical basis for radiation-induced segregation strongly suggests that this phenomenon is general and likely to occur in any alloy and even in metals with minor impurities.

Radiation-induced segregation may occur for two reasons. First, the presence of a high supersaturation of vacancies (and interstitials) enhances the mobility of impurities and solute elements. Equilibrium segregation which may be too sluggish to occur without irradiation may therefore be speeded up. The second reason for segregation is connected with the continuous flux of point defects to sinks. The associated atomic jump processes may transport preferentially certain solute elements leading to their enrichment or depletion at the sinks. The resulting compositional gradients are truly nonequilibrium gradients and require for their maintenance the continuous point defect fluxes to the sinks. But even for a continuous and constant irradiation, a truly stationary state may never be achieved for two reasons. First, the sink structure changes both in space and with irradiation time. The cause for the evolution of the sink structure is of course the well known bias for preferential absorption of interstitials at dislocations. Since the nonequilibrium segregation is coupled to the point defect fluxes to sinks, a continuous redistribution of solutes occurs with the microstructural evolution. A second reason is that the segregation itself will lead to a modification of the sink bias factors and therefore directly influence the microstructural evolution.

It is the main purpose of this paper to investigate the physical basis for the bias modification as produced by the radiation-induced segregation. This will be done by deriving the diffusion fluxes for interstitials and vacancies in an alloy with compositional gradients. Although explicit bias factors will not be derived in the present paper, it will nevertheless become evident that the new drift terms which appear will profoundly affect the bias factors of all sinks, i.e. voids and dislocations alike.

The previous work of Wolfer and Mansur [3] on the capture efficiency of coated voids is in light of the present work only a special case of bias modifications as produced by non-equilibrium segregation. In this previous work, the compositional gradient around voids was modeled by a discrete shell whose lattice parameter and elastic properties differed slightly from those of the surrounding matrix. The presence of this shell resulted in a significant change of the void bias factors as compared to those for bare voids, particularly when the void radius was very small. Recently, Si-Ahmed and Wolfer [4] have demonstrated that minute differences in either the lattice parameters or the shear moduli between shell and matrix can change the void nucleation rate by several orders of magnitude.

Because of the sensitivity of void nucleation to segregation-induced bias modifications, one must inevitably conclude that void formation and swelling is to a large degree dependent on, if not entirely determined by, the radiation-induced segregation and precipitation. This conclusion lends much support to the empirically derived hypothesis by Garner [5] that the microchemical evolution is one of the major factors which control the onset of swelling in austenitic stainless steels, and perhaps other alloys. This idea is deduced from extensive observations on segregation and precipitation that precedes and accompanies void swelling in type 304 and 316 stainless steels [6-11].

The effect of segregation on the diffusion fluxes of vacancies and interstitials is derived with the help of the linear theory of irreversible thermodynamics in Section 2. This derivation follows the approach of Marwick [12], and Chauvin [13] and Martin [14]. The various contributions to the drift terms in the diffusion fluxes are then examined in detail in Section 3, and numerical estimates are made in Section 4 for these contributions in the case of binary Fe-Ni alloys.

2. ATOM AND POINT DEFECT FLUXES

In order to keep matters simple we consider a substitutional binary alloy made up of atoms A and atoms B. Diffusion of both atoms may take place via the vacancy and the interstitialcy mechanisms. For the latter, an atom migrates as part of the dumbbell interstitial formed as a result of the radiation damage. Furthermore, we assume that no coupling exists between the atom fluxes J_{AV}, J_{BV} and J_{AI}, J_{BI} associated with the vacancy and interstitial migration. This assumption is justified since the atomic fractions of both vacancies and interstitials, x_V and x_I, are very small compared to one. Hence, the presence of vacancies does not affect the interstitial flux other than leading to recombination. This reaction is, however, taken into account in the rate equations which determine the global concentration of both vacancies and interstitials. In contrast, the equation to be derived for the fluxes of atoms and point defects applies to the local scale between sinks, i.e. to regions of "good" crystal.

If x_A and x_B denote the atomic fraction of A and B atoms in the alloy on substitutional places, then

$$x_A + x_B = 1 - x_V \cong 1 \ . \tag{1}$$

The fluxes of both atoms, J_A and J_B, and the fluxes of point defects, J_V and J_I, satisfy the condition

$$J_A + J_B = J_I - J_V \tag{2}$$

for any cross sectional area not intersecting a point defect sink. Based on the above assumption, the atom fluxes, J_A and J_B, are composed of two contributions, e.g.,

$$J_A = J_{AV} + J_{AI} \ , \tag{3}$$

and they are independent of each other and simply additive. The partial atomic currents are related to the point defect currents by

$$J_{AV} + J_{BV} = -J_V \tag{4}$$

and

$$J_{AI} + J_{BI} = J_I \ . \tag{5}$$

The driving forces for these currents are the local chemical potential gradients for the two atomic species and the two point defects. We define the chemical potentials in the conventional manner as

$$\mu_A = \mu_A^o + kT \ln(\gamma_A x_A) \tag{6}$$

$$\mu_B = \mu_B^o + kT \ln(\gamma_B x_B) \tag{7}$$

$$\mu_V = kT \ln(x_V/x_V^{eq}) \tag{8}$$

$$\mu_I = kT \ln(x_I/x_I^{eq}) \tag{9}$$

where μ_A^o and μ_B^o are the chemical potentials of the atoms in a reference state, γ_A and γ_B are the activity coefficients, and

$$x_V^{eq} = \exp(-G_V^f/kT) \tag{10}$$

$$x_I^{eq} = \exp(-G_I^f/kT) \tag{11}$$

are the thermodynamic equilibrium concentrations of vacancies and interstitials, respectively. It is assumed in the following that the Gibbs free energies for point defect formation, G_V^f and G_I^f, are functions of the local alloy composition and the local state of stress.

According to the linear thermodynamics of irreversible processes, the currents of atoms and point defects are in general linearly dependent on the gradients of all four chemical potentials [15,16]. However, based on the assumption above, the currents J_V, J_{AV}, and J_{BV} are independent of $\nabla\mu_I$, whereas the currents J_I, J_{AI}, and J_{BI} are independent of $\nabla\mu_V$. Furthermore, because the currents associated with vacancies are related by Eq. (4), there are only two independent currents among J_V, J_{AV}, and J_{BV}. Therefore, one may write [13]

$$J_{AV} = -L^{V}_{AA} \frac{1}{T} \nabla(\mu_A - \mu_V) - L^{V}_{AB} \frac{1}{T} \nabla(\mu_B - \mu_V) \tag{12}$$

$$J_{BV} = -L^{V}_{BB} \frac{1}{T} \nabla(\mu_B - \mu_V) - L^{V}_{AB} \frac{1}{T} \nabla(\mu_A - \mu_V) \ , \tag{13}$$

where the phenomenological coefficients L^{V}_{AA}, etc., are to be determined later. Similar equations can be written down for the partial interstitial current J_{AI} and J_{BI} except that they depend on the gradients $\nabla(\mu_A + \mu_I)$ and $\nabla(\mu_B + \mu_I)$.

The Gibbs-Duhem equation provides a further relationship that connects the chemical potential gradients according to

$$x_A \nabla\mu_A + x_B \nabla\mu_B + x_V \nabla\mu_V + x_I \nabla\mu_I = 0 \ . \tag{14}$$

For all practical situations of interest to high-temperature radiation damage, the point defect fractions x_V and x_I are orders of magnitude smaller than the atom fractions x_A and x_B even in case of dilute alloys. Therefore,

$$x_A \nabla\mu_A + x_B \nabla\mu_B \cong 0 \ , \tag{15}$$

which represents the traditional Gibbs-Duhem relationship for a binary alloy. Equation (15) allows us to eliminate one of the chemical potential gradients, say, $\nabla\mu_B$, and we obtain for the partial currents the expressions

$$J_{AV} = -(L^{V}_{AA} - \frac{x_A}{x_B} L^{V}_{AB}) \frac{1}{T} \nabla\mu_A + (L^{V}_{AA} + L^{V}_{AB}) \frac{1}{T} \nabla\mu_V \tag{16}$$

$$J_{BV} = (\frac{x_A}{x_B} L_{BB}^V - L_{AB}^V) \frac{1}{T} \nabla\mu_A + (L_{AB}^V + L_{BB}^V) \frac{1}{T} \nabla\mu_V . \qquad (17)$$

In order to express the partial currents in terms of concentration gradients we make use of the defining equations for the chemical potentials, Eqs. (6) to (9), and we find

$$\nabla\mu_A = kT \frac{\alpha_A}{x_A} \nabla x_A \qquad (18)$$

$$\nabla\mu_V = kT \frac{1}{x_V} \nabla x_V - kT \frac{\xi_{VA}}{x_A} \nabla x_A \qquad (19)$$

where

$$\alpha_A = 1 + \frac{\partial \ln \gamma_A}{\partial \ln x_A} \qquad (20)$$

is the thermodynamic factor and

$$\xi_{VA} = \frac{\partial \ln x_V^{eq}}{\partial \ln x_A} = - \frac{x_A}{kT} \frac{\partial G_V^f}{\partial x_A} , \qquad (21)$$

i.e. a factor proportional to the rate of change of the vacancy formation energy with the alloy composition.

It should be noted that it was assumed in Eq. (18) that the chemical potential μ_A or the activity coefficient γ_A is independent of the vacancy and interstitial concentrations. Although this may not be a legitimate assumption in a global sense it is valid when applied to crystal regions of dimensions less than the average distance between defects. Again, as pointed out above, the expressions for the fluxes are then valid only for these regions of "good" crystal in between defect sinks.

The partial atomic fluxes can now be written as

$$J_{AV} = -k[(\frac{L^V_{AA}}{x_A} - \frac{L^V_{AB}}{x_B})\alpha_A + (L^V_{AA} + L^V_{AB})\frac{\xi_{VA}}{x_A}]\nabla x_A + k(L^V_{AA} + L^V_{AB})\frac{1}{x_V}\nabla x_V \qquad (22)$$

$$J_{BV} = -k[(\frac{L^V_{AB}}{x_A} - \frac{L^V_{BB}}{x_B})\alpha_A + (L^V_{AB} + L^V_{BB})\frac{\xi_{VA}}{x_A}]\nabla x_A + k(L^V_{AB} + L^V_{BB})\frac{1}{x_V}\nabla x_V \qquad (23)$$

and the vacancy flux as

$$J_V = -k[L^V_{AA} + 2L^V_{AB} + L^V_{BB}]\frac{1}{x_V}\nabla x_V + k[(\frac{L^V_{AA}}{x_A} - \frac{L^V_{AB}}{x_B} - \frac{L^V_{BB}}{x_B} + \frac{L^V_{AB}}{x_A})\alpha_A + (L^V_{AA} + 2L^V_{AB} + L^V_{BB})\frac{\xi_{VA}}{x_A}]\nabla x_A . \qquad (24)$$

According to Manning [15], the phenomenological coefficient can be related to the tracer diffusion coefficients D^*_{AV} and D^*_{BV} and the correlation factor f_V for the vacancy mechanism of diffusion; the latter is $f_V = 0.78145$ for the fcc lattice. The relationships are

$$kL^V_{AA} = Nx_AD^*_{AV}(1 + x_AD^*_{AV}Q_V) \qquad (25)$$

$$kL^V_{BB} = Nx_BD^*_{BV}(1 + x_BD^*_{BV}Q_V) \qquad (26)$$

$$kL^V_{AB} = Nx_Ax_BD^*_{AV}D^*_{BV}Q_V \qquad (27)$$

where

$$Q_V = (\frac{1}{f_V} - 1)/(x_AD^*_{AV} + x_BD^*_{BV}) \qquad (28)$$

and N is the number of atomic sites per unit volume. Therefore,

$$k(L_{AA}^{V} + 2L_{AB}^{V} + L_{BB}^{V}) = \frac{N}{f_V}(x_A D_{AV}^{*} + x_B D_{BV}^{*}) = N x_V D_V = C_V D_V \tag{29}$$

where C_V is the vacancy concentration and D_V the diffusion coefficient for vacancy migration. This latter assignment is of course made to cast the first term of Eq. (24) into the familiar form, namely $D_V \nabla C_V$. The relationships expressed in Eq. (29) further suggest the following definition of the atomic diffusivities,

$$D_{AV} = D_{AV}^{*}/(x_V f_V) \tag{30}$$

$$D_{BV} = D_{BV}^{*}/(x_V f_V) \ , \tag{31}$$

as introduced by Wiedersich et al. [17] (and denoted by d_{AV} and d_{BV} in their paper).

The fluxes can finally be expressed in terms of concentration gradients as

$$J_{AV} = -D_{AV}^{*}\{[1 + (D_{AV}^{*} - D_{BV}^{*})x_A Q_V]\alpha_A + (\frac{\xi_{VA}}{f_V})\}\ \nabla C_A + D_{AV} x_A \nabla C_V \tag{32}$$

$$J_{BV} = +D_{BV}^{*}\{[1 - (D_{AV}^{*} - D_{BV}^{*})x_B Q_V]\alpha_A - (\frac{x_B}{x_A})(\frac{\xi_{VA}}{f_V})\}\ \nabla C_A + D_{BV} x_B \nabla C_V \tag{33}$$

and

$$J_V = -D_V \nabla C_V - \frac{D_V C_V}{kT}\frac{\partial G_V^f}{\partial C_A}\nabla C_A + (D_{AV} - D_{BV})\alpha_A x_V \nabla C_A \ . \tag{34}$$

Since the vacancy formation energy, G_V^f, is a function of the local alloy composition, we must likewise presume a dependence for the vacancy migration energy. Hence, if D_V^o denotes a constant pre-exponential factor, then

$$D_V = D_V^o \exp(-G_V^m/kT) \tag{35}$$

where $G_V^m(x_A)$ is the local Gibbs free energy for vacancy migration.

Equation (34) may then be cast in the alternate form

$$\boxed{J_V = -\nabla(D_V C_V) - \frac{D_V C_V}{kT} \nabla(G_V^f + G_V^m) + (D_{AV} - D_{BV})\alpha_A x_V \nabla C_A \ .} \tag{36}$$

The above derivation for the vacancy flux can be repeated along the same lines for the interstitial flux with two differences. First, as seen from Eqs. (4) and (5), the interstitial flux is in the same direction as the partial atomic interstitialcy currents. Second, this results in a change of sign in Eqs. (12) and (13) such that the interstitialcy currents J_{AI} and J_{BI} are now driven by the chemical potential gradients $\nabla(\mu_A + \mu_I)$ and $\nabla(\mu_B + \mu_I)$, and they are proportional to different phenomenological coefficients L_{AA}^I, etc. The latter can again be related to tracer diffusion coefficients D_{AI}^* and D_{BI}^* or interstitialcy diffusivities D_{AI} and D_{BI} according to equations analogous to the Eqs. (25) to (31).

The atomic interstitialcy fluxes are then found to be

$$J_{AI} = -D_{AI}^* \left\{[1 + (D_{AI}^* - D_{BI}^*)x_A Q_I]\alpha_A - \left(\frac{\xi_{IA}}{f_I}\right)\right\} \nabla C_A - D_{AI} x_A \nabla C_I \tag{37}$$

$$J_{BI} = D^*_{BI} \{[1 - (D^*_{AI} - D^*_{BI})x_B Q_I]\alpha_A + (\frac{x_B}{x_A})(\frac{\xi_{IA}}{f_I})\} \nabla C_A - D_{BI} x_B \nabla C_I \qquad (38)$$

and the interstitial flux is

$$\boxed{J_I = -\nabla(D_I C_I) - \frac{D_I C_I}{kT} \nabla(G^f_I + G^m_I) - (D_{AI} - D_{BI})\ \alpha_A x_I \nabla C_A} \qquad (39)$$

Equations (36) and (39) represent the basis for the segregation-induced bias modifications. The following section is therefore devoted to a more detailed discussion of the drift terms, i.e. the last two terms contained in Eqs. (36) and (39). When the discussion applies equally to interstitials and vacancies, the indices "I" and "V" will be omitted.

3. THE CONTRIBUTIONS TO THE DRIFT

A. Overview

The drift terms in Eqs. (36) to (39) are responsible for the bias. Although only two drift terms appear explicitly in the flux equations for the point defects, there are in fact more contributions as illustrated in Fig. 1. The various contributions will be discussed briefly in the following, and more extensively in later sections.

Let us consider first the drift term proportional to the gradient of the saddle point energy, $\nabla(G^f + G^m)$. The energy $(G^f + G^m)$ represents the total Gibbs free energy when a point defect is created in its saddle-point configuration, and it can be broken down into the following parts:

$$G^S = G^f + G^m = \overline{G}^S + U^{BR} + U^I + U^\sigma + U^C\ . \qquad (40)$$

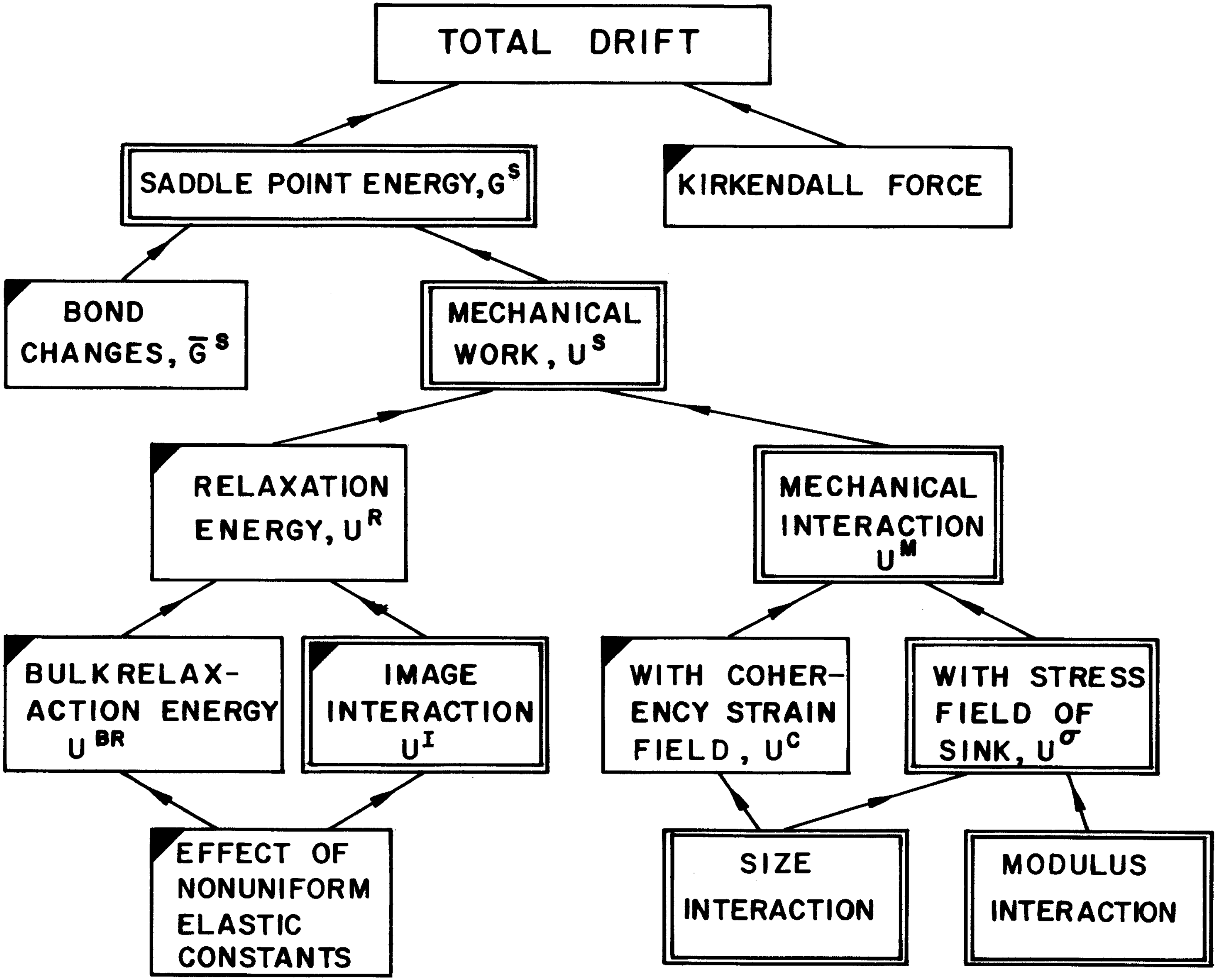

Figure 1 The various contributions to the total drift force on point defects in an alloy with compositional gradients.

The first term, $\bar{G}^S$, arises from the chemical bond changes when the point defect is introduced into an ideal lattice which is free of stress, and with all atoms confined to remain in their ideal lattice positions. $\bar{G}^S$ depends then only on the local composition.

The remaining terms in Eq. (40) arise in conjunction with the relaxation of atoms to new equilibrium positions, giving rise to the strain field of the point defect. All these terms represent therefore the total mechanical work U^S associated with the creation of a point defect. This mechanical work consists in turn of the so-called relaxation energy

$$U^R = U^{BR} + U^I \qquad (41)$$

and of the mechanical interaction energy

$$U^M = U^\sigma + U^C \ . \qquad (42)$$

The relaxation energy U^R of a point defect is equal to the elastic strain energy associated with the displacement field of the point defect. U^R depends on the position of the point defect with regard to free surfaces and interfaces. When the point defect is far from any free surface or interface, it consists of a single contribution, called henceforth the bulk relaxation energy U^{BR}. Its evaluation will be given below for a medium with spatially varying elastic properties. In the vicinity of free surfaces, or interfaces separating regions of distinctly different elastic properties, an image interaction U^I must be added to U^{BR}.

The contribution to the mechanical interaction energy U^M which has been considered in the past as the only source of the bias is U^σ. (Exceptions are the investigations in Refs. 3, 4, and 12.) This energy arises from the interaction of the point defect with the stress field of the sink, and it is composed of two parts: the size interaction which is linear in the stresses, and the modulus interaction which depends on the second power in the stresses.

Segregation may affect this mechanical interaction energy U^M in two ways. First, compositional variations may lead to variations in the local lattice parameter. However, since regions with different lattice parameters must remain coherent, additional strains are produced which superimpose on the strains created by the sink itself. This results in a coherency strain energy U^C which will be derived below. The second effect is associated with the nonuniform elastic properties which modify the stress field of the sink in the original medium with uniform elastic properties. For small changes in the elastic properties, however, this effect is negligible when compared to the original strain field of the sink such as the one of an edge dislocation.

All the contributions to the saddle-point energy G^S combine and relate to each other in a manner indicated in Fig. 1. In a material with uniform composition and therefore uniform properties, only those energies or effects contribute to G^S which are indicated by double frames in Fig. 1. The additional effects and contributions caused by segregation are marked by corner triangles in Fig. 1.

The following sections are now devoted to a more detailed treatment of the drift contributions, particularly of those which arise in conjunction with segregation. However, the other contributions are also discussed briefly for the sake of completeness.

B. The Relaxation Energy

Consider first a medium with uniform elastic constants. For simplicity we assume that the medium is also elastically isotropic with bulk modulus $\overline{\kappa}$ and shear modulus $\overline{\mu}$. As shown in Appendix A, the strain energy of an isotropic point defect with relaxation volume v is given by

$$\overline{U}^{BR} = \frac{2\overline{\kappa}\,\overline{\mu}}{3\overline{\kappa} + 4\overline{\mu}} \frac{v^2}{\Omega} \tag{43}$$

where Ω is the atomic volume, and the point defect is far from any free surfaces.

Suppose now that the medium has a spatially varying composition and therefore varying elastic constants given by

$$\mu(\vec{r}) = \overline{\mu} + \delta\mu(\vec{r}) \quad \text{and} \quad \kappa(\vec{r}) = \overline{\kappa} + \delta\kappa(\vec{r}) \tag{44}$$

where $\overline{\mu}$ and $\overline{\kappa}$ are average values. If $\delta\mu/\overline{\mu}$ and $\delta\kappa/\overline{\kappa}$ vary only by small amounts over distances on the order of a few lattice parameters, then the change in the relaxation energy of the point defect is given by

$$\delta U^{BR} \cong \left\{\frac{3\overline{\kappa}}{3\overline{\kappa} + 4\overline{\mu}} \frac{\delta\mu}{\overline{\mu}} + \frac{4\overline{\mu}}{3\overline{\kappa} + 4\overline{\mu}} \frac{\delta\kappa}{\overline{\kappa}}\right\} \overline{U}^{BR} . \tag{45}$$

As shown in Appendix A, this approximation for δU^{BR} represents in fact a correct upper bound, and it is exact to linear order in $\delta\mu$ and $\delta\kappa$.

With this linear approximation, we can define the spatially varying relaxation energy simply as

$$U^{BR}(\vec{r}) = \bar{U}^{BR} + \delta U^{BR}(r) = \frac{2\kappa(\vec{r})\mu(\vec{r})}{3\kappa(\vec{r}) + 4\mu(\vec{r})} \frac{v^2}{\Omega} . \qquad (46)$$

It should be noted that the relaxation volume v may also depend on the local alloy composition. However, there is virtually no information available regarding this possibility, and we shall have to disregard it.

C. The Image Interaction

The above Eq. (45) becomes invalid when the elastic moduli change abruptly as in cases where the point defect approaches a free surface (beyond which the elastic moduli vanish) or a precipitate interface (beyond which the elastic moduli assume substantially different values).

Close to these surfaces, the relaxation energy U^R changes by an additional amount, the so-called image interaction U^I. A detailed evaluation and discussion of this interaction has been given by Wolfer and Mansur [3,18] for the case of a spherical void. When the segregation around voids produces only small variations in the elastic properties, the image interaction can be approximated by the expression [3]

$$U^I(r) = - \frac{(1 + \nu)^2}{36\pi(1 - \nu)} \frac{\bar{\mu}v^2}{a^3} \left[\left(\frac{r}{a} - 1\right)^3 + \frac{7 - 5\nu}{30} \left(\frac{r}{a} - 1\right)^6\right]^{-1} \qquad (47)$$

where a is the void radius, r the distance to the void center, and ν is Poisson's ratio.

If the segregation produces a distinct coherent precipitate shell around the void, the more complex expression [18] is required for the image interaction U^I.

D. The Coherency Strain Interaction

The lattice parameter of an alloy is in general a function of the composition. With a non-uniform composition, the local lattice parameter $a_o(\vec{r})$ would deviate from the average value $\bar{a}_o$ by the relative amount

$$\eta(\vec{r}) = \frac{a_o(\vec{r}) - \bar{a}_o}{\bar{a}_o} \tag{48}$$

if the crystal were in fact not subject to coherency strains. The latter can be computed from the function $\eta(\vec{r})$ as shown in Appendix B. Based on the size-interaction with this coherency strain field, the interaction energy is found to be given by

$$U^C(\vec{r}) = \mu \frac{\Omega}{V} \bar{U}^{BR} \eta(\vec{r}) \ . \tag{49}$$

In the derivation of U^C given in Appendix B, we assumed constant elastic properties in order to obtain a theory consistent to first order in the compositional gradients as required by the linear theory of irreversible thermodynamics. In other words, terms are neglected which are of the order of $\delta\mu \cdot \eta$ and $\delta\kappa \cdot \eta$.

E. The Mechanical Interaction with the Stress Field of Sinks

If a sink produces a stress-field $\sigma_{ij}(\vec{r})$, the point defect interacts with it according to the expression [19,20]

$$U^\sigma = -\frac{1}{3} v\sigma_{ii} + \frac{\alpha^K}{18\bar{\kappa}^2} \sigma_{ii}\sigma_{jj} + \frac{\alpha^G}{4\bar{\mu}^2} {'\sigma_{ij}} {'\sigma_{ij}} \ . \tag{50}$$

Here, repeated indices indicate a summation,

$$'\sigma_{ij} = \sigma_{ij} - \frac{1}{3}\,\delta_{ij}\sigma_{\kappa\kappa}$$

is the deviatoric stress tensor, and α^K and α^G are the elastic polarizabilities of the point defect. The above interaction energy is generally the one considered in bias calculations, and often only the first term, the size-interaction, is retained, whereas the remaining modulus interaction is neglected.

The interaction U^σ has been evaluated previously for both dislocations [20] and voids [21], and its effect on the bias factors for these sinks has been derived.

F. Energy Associated with Bond Changes

Although it is conceptually simple to separate the formation energy of a point defect into the two parts, $\overline{G}^S$ and $\overline{U}^{BR}$, it is only the sum that can be measured experimentally at least in the case of vacancies. Here, the sum represents the activation energy for self-diffusion. The relaxation energy $\overline{U}_V^{BR}$ for vacancies is typically on the order of 0.1 eV to 0.5 eV (1.6×10^{-20} to 8×10^{-20} J), whereas the corresponding value $\overline{U}_I^{BR}$ for the self-interstitial is a factor of about 20 larger. Therefore, the formation energy of a point defect in its stable or saddle-point configuration consists mainly of the contribution $\overline{G}_V^S$ due to bond changes in the case of vacancies, but in the case of interstitials, the relaxation energy $\overline{U}_I^{BR}$ is the main contributor. As a result, we shall assume that $\overline{G}_I^S$ can be neglected compared to $\overline{U}_I^{BR}$. For the vacancy, on the other hand, we shall equate the sum $(\overline{G}_V^S + \overline{U}_V^{BR})$ to the activation energy for self-diffusion, and utilize experimental data when available. Then

$$\nabla[(\bar{G}_V^S + \bar{U}_V^{BR})/kT] = -\nabla[\ln D_{SD}] \tag{51}$$

where D_{SD} is the self-diffusion coefficient. If D_{AV}^{o*} and D_{BV}^{o*} are the tracer diffusion coefficients measured at thermal equilibrium conditions, then Eq. (29) gives

$$D_{SD} = \frac{1}{f_V}\,[x_A D_{AV}^{o*} + x_B D_{BV}^{o*}] \tag{52}$$

where both tracer diffusion coefficients are in general further dependent on the alloy composition.

G. Kirkendall Force

The last terms in Eqs. (36) and (39) represent what Marwick [12] calls the Kirkendall flux. It can be written as

$$[\mp \frac{DC}{kT}][\frac{(D_A^* - D_B^*)\alpha_A}{x_A D_A^* + x_B D_B^*}\,kT\nabla x_A]$$

where the upper (lower) sign holds for the interstitial (vacancy) Kirkendall flux. The second factor in the Kirkendall flux may now be interpreted as a drift force, which we shall call henceforth the Kirkendall force

$$\vec{F}_K = \pm\,\frac{(D_A^* - D_B^*)\alpha_A}{x_A D_A^* + x_b D_B^*}\,kT\nabla x_A\ . \tag{53}$$

The factor containing the tracer diffusion coefficients can be related to measurable quantities under thermal equilibrium conditions for the case of vacancies. Although D^*_{AV} and D^*_{BV} represent the tracer diffusion coefficients under irradiation, they are connected with the coefficients for thermal equilibrium according to

$$D^*_{AV} = (x_V/x_V^{eq})D^{o*}_{AV} \quad \text{and} \quad D^*_{BV} = (x_V/x_V^{eq})D^{o*}_{BV} \quad . \tag{54}$$

Hence, the Kirkendall force for vacancies can also be written as

$$\vec{F}_{KV} = -K_V kT\nabla x_A = -\frac{(D^{o*}_{AV} - D^{o*}_{BV})\alpha_A}{x_A D^{o*}_{AV} + x_B D^{o*}_{BV}} kT\nabla x_A \tag{55}$$

where the Kirkendall force coefficient K_V can now be evaluated with measured tracer diffusion coefficients and measured thermodynamic data. An example will be given below.

Tracer diffusion coefficients for interstitialcy migration must, however, be obtained under radiation conditions, and no experimental data is yet available. Furthermore, under irradiation, diffusion of tracer atoms would occur both via the vacancy and the interstitialcy mechanisms, and only the sum $(D^*_{AV} + D^*_{AI})$ could be obtained. By a separate measurement of the equilibrium tracer diffusion coefficient D^{o*}_{AV} and a knowledge of the vacancy concentrations both with and without irradiation, the tracer diffusion coefficient D^*_{AI} could be isolated. Similar measurements would also be required to obtain D^*_{BI}.

4. MAGNITUDE OF THE DRIFT TERMS FOR BINARY Fe-Ni ALLOYS

Having discussed the physical origin of the various drift contributions, estimates for their magnitude will now be provided. In view of the extensive data base available for void formation in austenitic stainless steels, we select the face-centered cubic binary alloys of iron and nickel. Although no attempt will be made here to establish a connection between radiation-induced segregation, segregation-induced bias modifications, and the dramatic dependence of void swelling on the nickel content in the austenitic series of alloys, this connection is certainly our ultimate goal and motivation for the present investigation. It will furthermore become apparent that more data on fundamental parameters for these alloys must be obtained before this connection can either be firmly established or rejected.

Let us first consider the various contributions to the mechanical interaction energy. For the following estimates, relaxation volumes of $v_I = 1.4\ \Omega$ and $v_V = -0.2\ \Omega$, and shear polarizabilities of $\alpha_I^G = -2.73 \times 10^{-17}$ J and $\alpha_V^G = -0.27 \times 10^{-17}$ J were selected for the interstitial and vacancy, respectively. An average shear modulus of $\overline{\mu} = 10^5$ MPa and a Poisson's ratio of 0.3 were chosen. Using the expressions given above as well as the one derived earlier [20] for the interaction energy U^σ between an edge dislocation and a point defect, values as given in Table 1 are obtained. Note that the interaction energies are the differences between the potential energies of the point defect far from the sink and near the sink. Negative values indicate therefore an attraction of the point defect, positive values a repulsion. It is seen that segregation resulting in a 3% elastic modulus change or in a 0.4% change in lattice parameter can change the interaction energy of an interstitial with the sink by amounts comparable to its interaction energy it has at a distance of 10 b from an edge dislocation. Local changes of shear modulus or lattice parameter of the above magnitude can easily be obtained with nickel segregation at sinks. For example, Marwick et al. [22] found that in a high nickel alloy of about 35% average nickel concentration, local concentrations of more than 54% nickel were obtained near voids. Similar obser-

Table 1. Typical Values for Mechanical Interaction Energies Associated with the Bias

Energy* in eV and in (10^{-21} J)	Interstitial	Vacancy
U^{σ} at a distance of 10 b from an edge dislocation above (upper signs) and below (lower signs) the glide plane	±0.25(±40)	∓0.05(∓8)
U^{I} at a distance from the void surface of 2 b	-0.25(-40)	-0.025(-4)
5 b	-0.005(-0.8)	-0.0005(-0.08)
δU^{BR} for a shear modulus change of ±1%	±0.08(±13)	±0.002(±0.32)
U^{C} for a lattice parameter change of ±0.1%	±0.06(±9.6)	∓0.008(∓1.3)

*Negative values imply a reduction of the point defect's energy relative to its average value or its value in an ideal and uniform crystal.

vations were made by Brager and Garner [23] in 316 SS and by Thomas [24] on voids in Fe-Ni-Cr alloys.

Nickel concentration has a strong effect on both the shear modulus and the lattice parameter, as can be seen from Figs. 2 and 3. The data shown in Fig. 2 are computed values for the shear modulus of a polycrystal, based on measured elastic moduli for single crystals [25]. The lattice parameters shown in Fig. 3 are due to Owen and Yates [26].

For an estimate of the drift force $\nabla \bar{G}_V^S$ and of the Kirdendall force, the diffusion measurements and thermodynamic data of Million et al. [27] are utilized. They have obtained tracer diffusion coefficients at temperatures between 985°C and 1305°C in binary Fe-Ni alloys, and fitted the results to the following equations:

$$\log_{10} D_{Ni}^{o*} = 0.537 - \frac{15152}{T} - x_{Fe} \left(0.488 - \frac{340}{T}\right) \tag{56}$$

$$\log_{10} D_{Fe}^{o*} = -0.142 - \frac{14561}{T} + x_{Ni} \left(1.106 - \frac{993}{T}\right) . \tag{57}$$

Here the temperature is in Kelvin and the diffusion coefficients in cm^2/s. If we use Eq. (52) to compute the self-diffusion coefficient and then the quantity $(-kT \ln D_{SD})$, we obtain the activation free energy required in Eq. (51). Since we only need the gradient of this quantity, $-kT \ln D_{SD}$ was normalized such that it gives the same value for $x_{Ni} = 1$. The results are shown in Fig. 4. It is seen that $(\bar{G}_V^S + \bar{U}_V^{BR})$ varies between $x_{Ni} = 0.35$ and $x_{Ni} = 0.54$ by 0.0075 eV or less within the temperature range of swelling. This must be compared with δU_V^{BR} which is about 0.008 eV for a 3% change in the shear

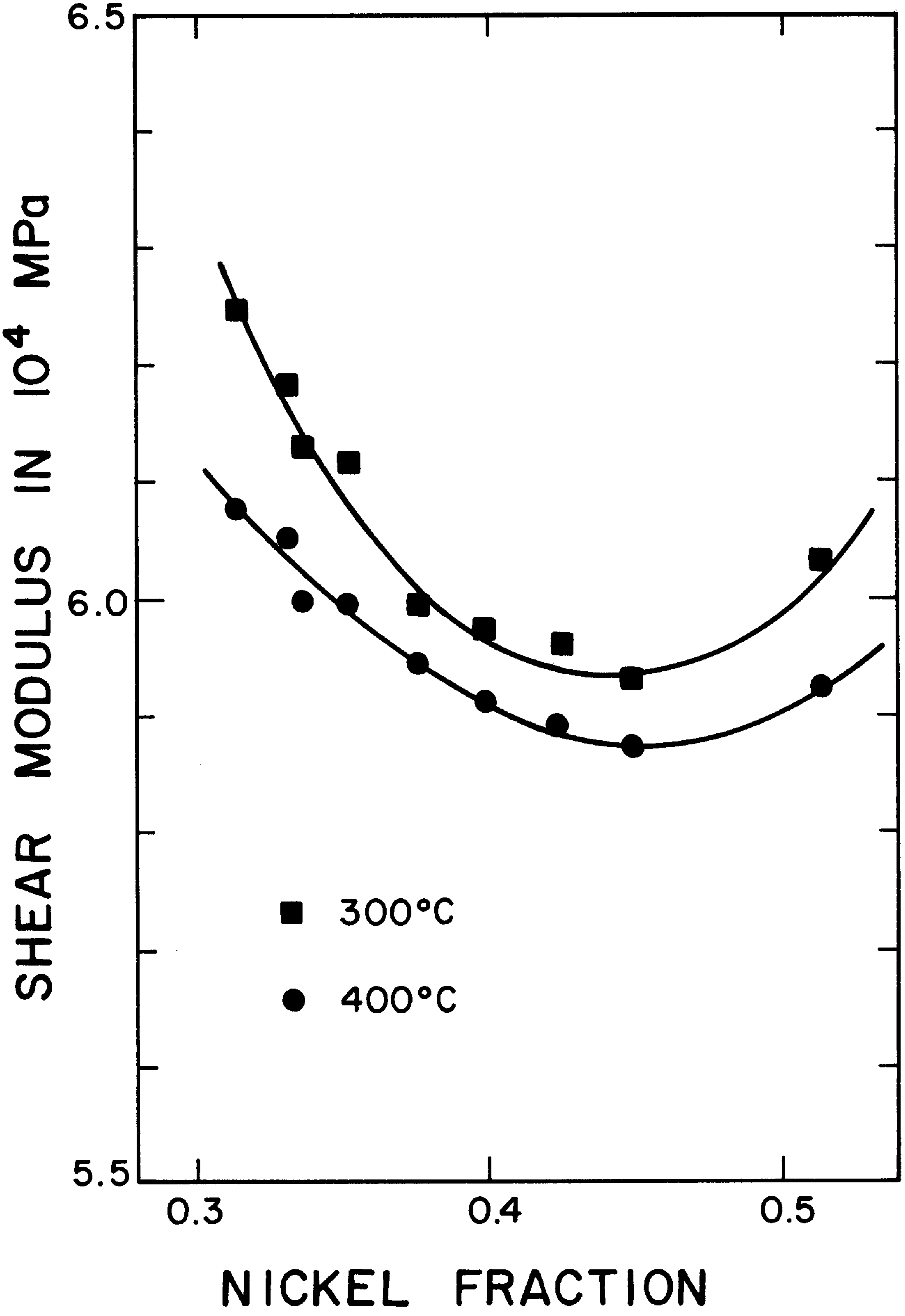

Figure 2 Shear modulus variation in binary alloys of iron and nickel [25].

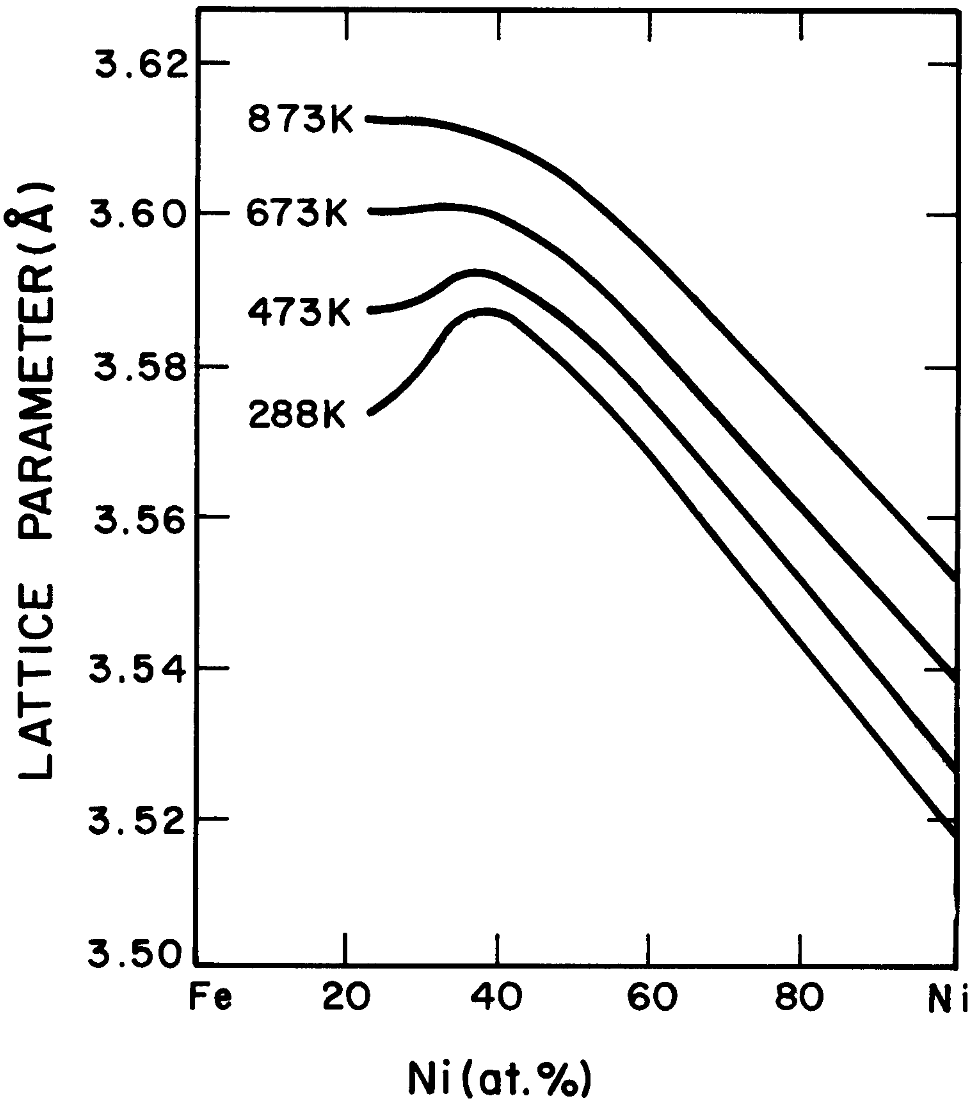

Figure 3 Lattice parameter variation in binary alloys of iron and mickel [26].

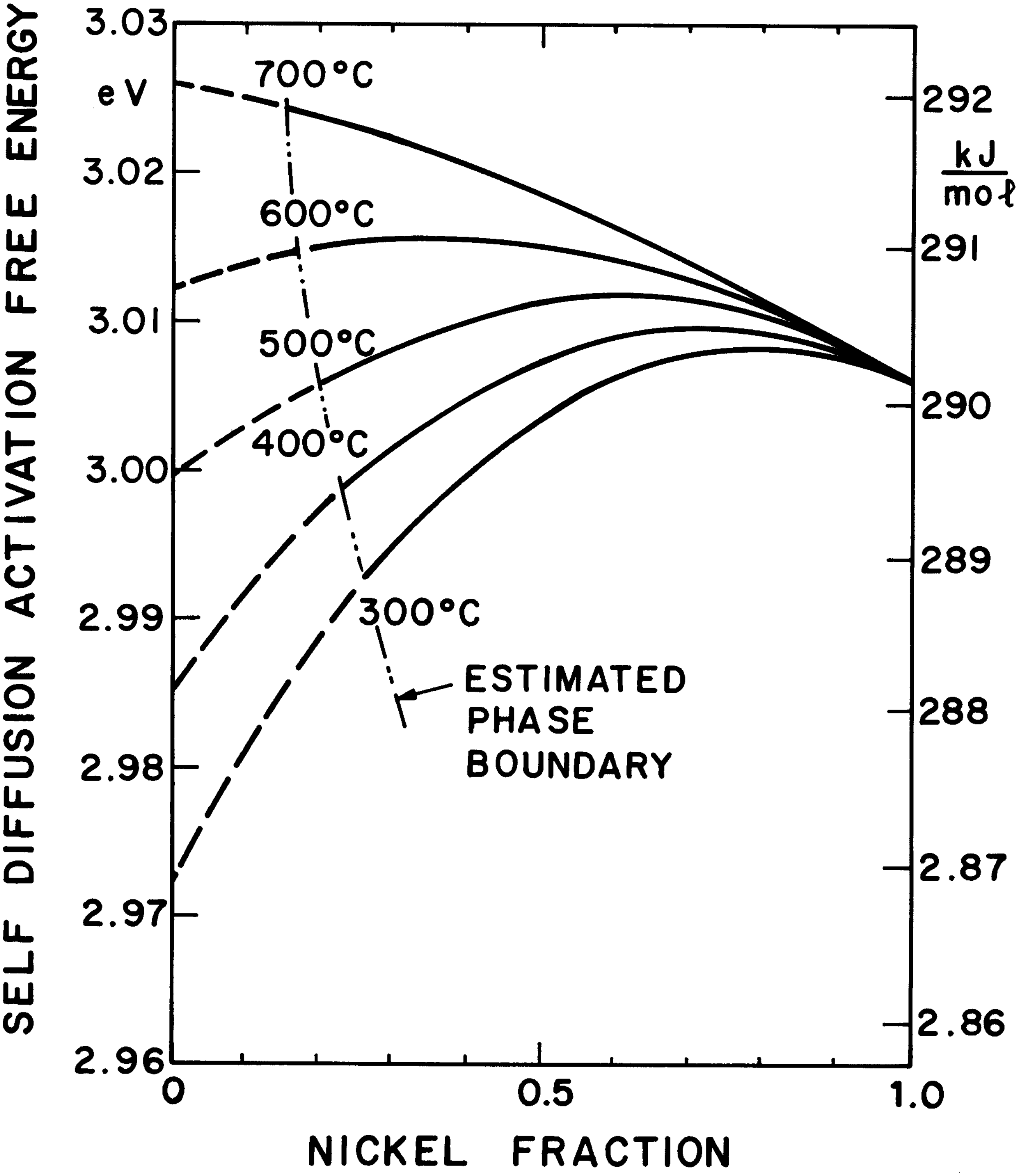

Figure 4 Activation energy for self-diffusion in binary alloys of iron and nickel.

modulus. Therefore, both estimates of the change in the saddle-point energy of a vacancy lead to roughly the same order of magnitude.

Finally, we estimate the Kirkendall force for both vacancies and interstitials. For the vacancies we can utilize again the above expressions for the tracer diffusion coefficients. In addition, we require the thermodynamic factor

$$\alpha = 1 + \frac{d\ln \gamma_{Ni}}{d\ln x_{Ni}} .$$

Million et al. [27] have obtained data for the activity coefficient γ_{Ni} in the temperature range of 950°C to 1250°C, and expressed the results in the form

$$\ln \gamma_{Ni} = a + bx_{Ni} + cx_{Ni}^2 + dx_{Ni}^3 \tag{56}$$

where a, b, c, and d are temperature dependent parameters. Since $\ln \gamma_{Ni} = 0$ and $\alpha = 1$ for $x_{Ni} = 1$, the four constants are related by $a + b + c + d = 0$ and $b + 2c + 3d = 0$.

Figure 5 shows the values obtained by Million et al. [27] for the parameters b and d, together with our extrapolation to lower temperatures. With these extrapolated parameters, the thermodynamic factor is as shown in Fig. 6. The dotted curve is based on an alternate measurement at a temperature of 1236°C, also performed by Million et al. [27]. Included in this figure is also a result based on measurements by Tanji et al. [28]. It is seen that measurements of activity coefficients in the Fe-Ni alloys are not yet very satisfactory. Nevertheless, for the present purpose of estimating the

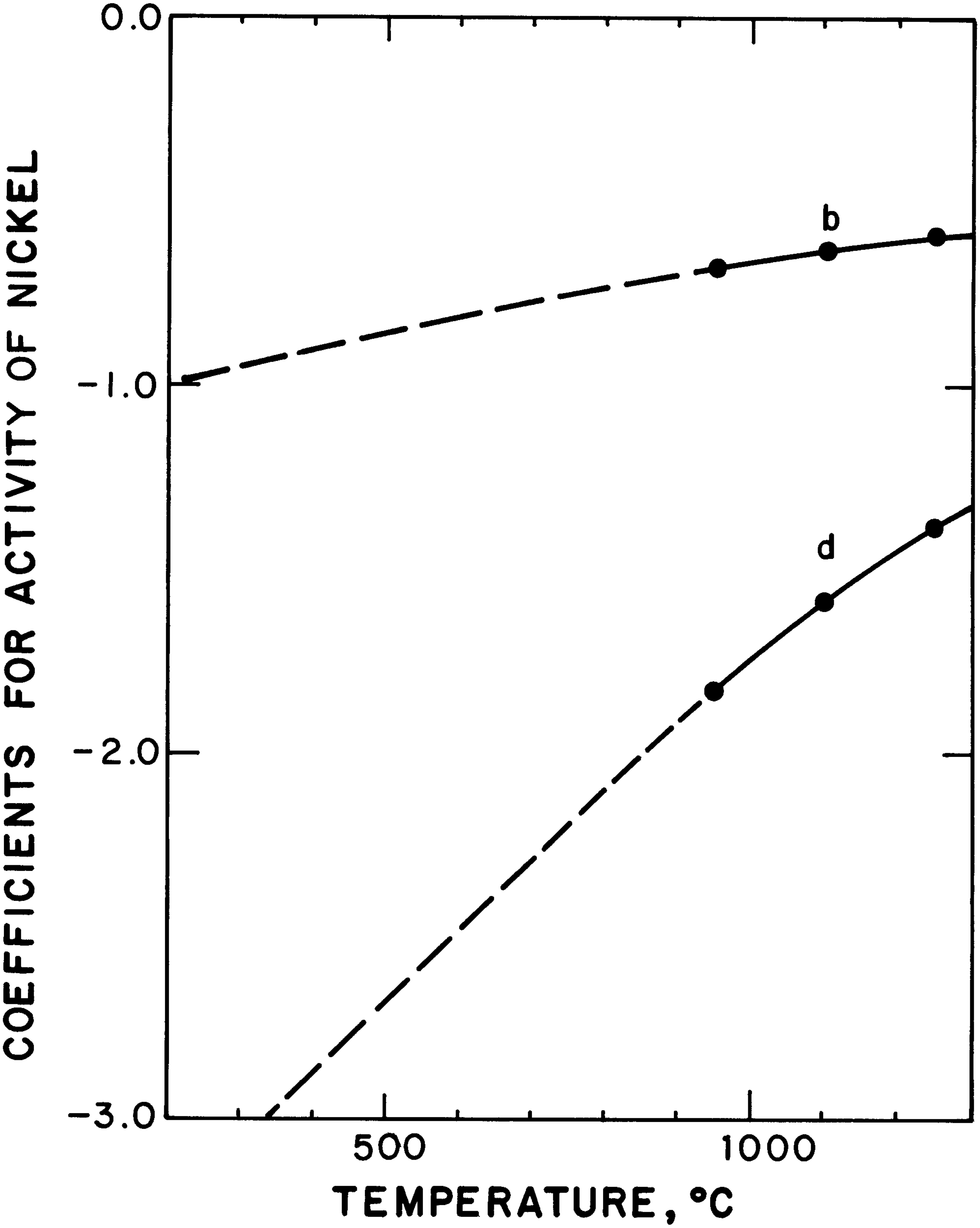

Figure 5 Temperature dependence of the coefficients in Eq. (56) for the activity coefficient.

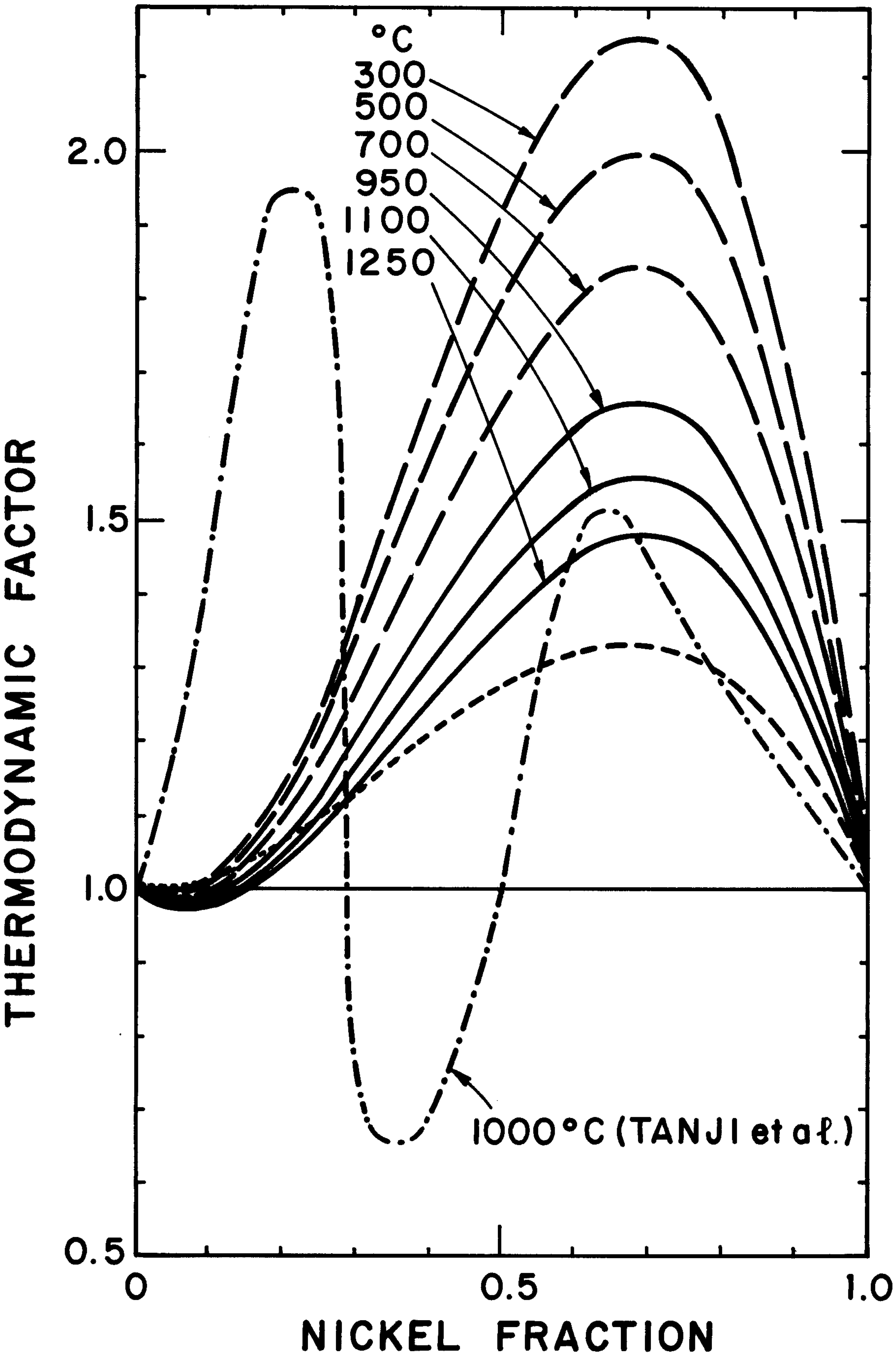

Figure 6 The thermodynamic factor for binary alloys of iron and nickel.

Kirkendall force on vacancies, the results of Million et al. will provide a convenient correlation.

The Kirkendall force coefficient K_V for vacancies is shown in Fig. 7, and it is found to vary between -0.5 and 1, depending on temperature and alloy composition. According to Eqs. (36) and (55), $(-D_V C_V K_V \nabla x_{Ni})$ is the Kirkendall contribution to the vacancy drift. Therefore, when the coefficient K_V shown in Fig. 7 is negative, the vacancies are attracted toward higher nickel concentrations. It is seen from Fig. 7 that this is the case when nickel segregation occurs at sinks in alloys with nickel content less than about 35%. Conversely, in alloys with more than 35% nickel, vacancies will be repelled by sinks with nickel segregation.

The Kirkendall force integrated over a nickel variation of about 20% can give rise to a potential energy change of about 0.015 eV at 300°C and of about 0.003 eV at 700°C. Therefore, at the lower irradiation temperature, the Kirkendall force on the vacancy can be comparable to the mechanical interaction force exerted by the dislocation stress field. As a result, the Kirkendall force is significant with regard to vacancy bias factors.

As there are no tracer diffusion coefficients available for diffusion by the interstitialcy mechanism we shall assume that the saddle-point energies for nickel and iron migration as part of the dumbbell interstitial differ by 0.05 eV. Using the same thermodynamic factor as before, the Kirkendall force coefficient K_I for interstitials is as shown as in Fig. 8.

Since the Kirkendall drift has the opposite sign for the interstitial flux as compared to the vacancy flux, a positive coefficient K_I implies that interstitials are attracted towards higher nickel concentration. This is the case when nickel is the faster diffusing species when migrating as part of a

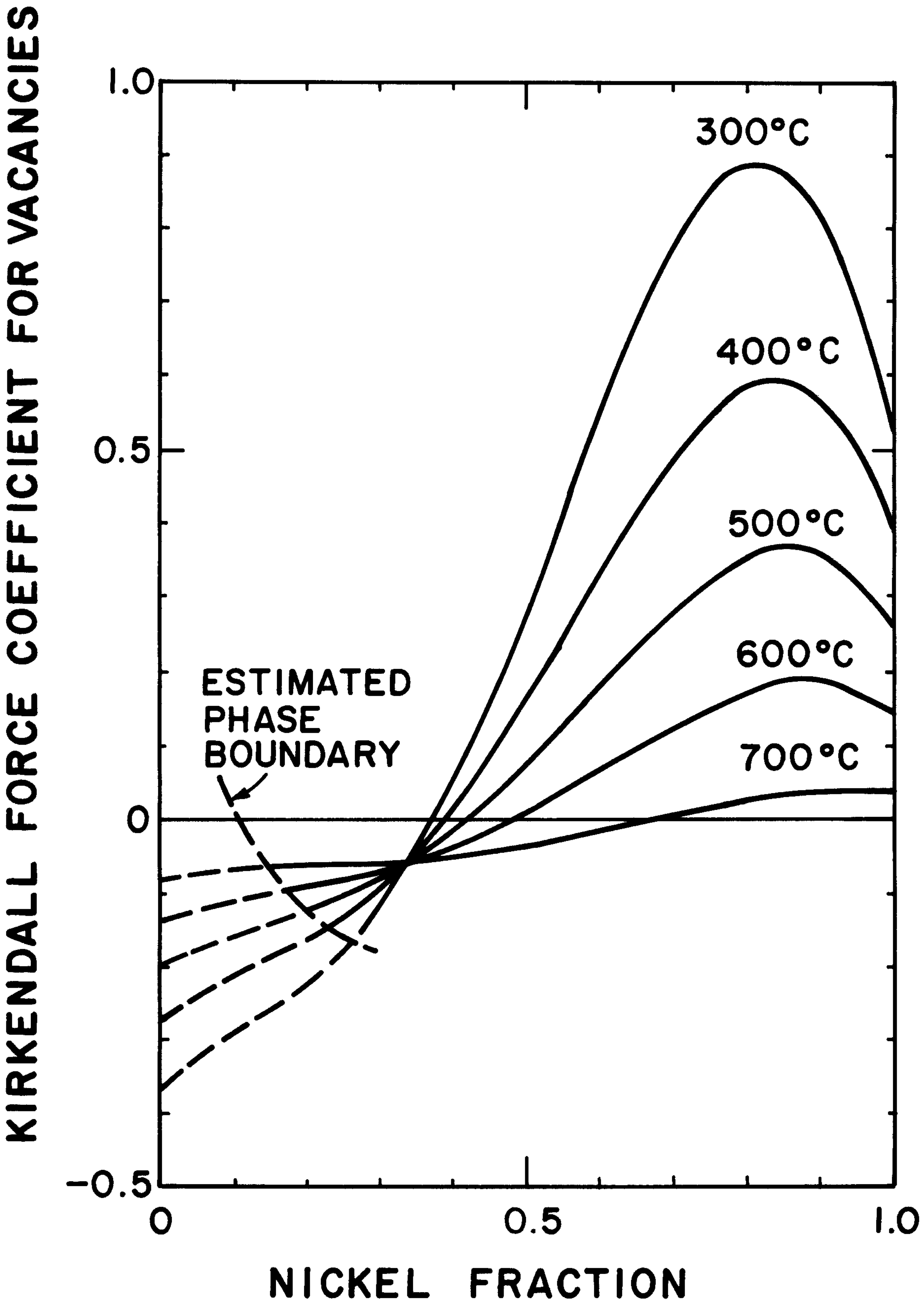

Figure 7 Predicted Kirkendall force coefficient for vacancies in binary alloys of iron and nickel.

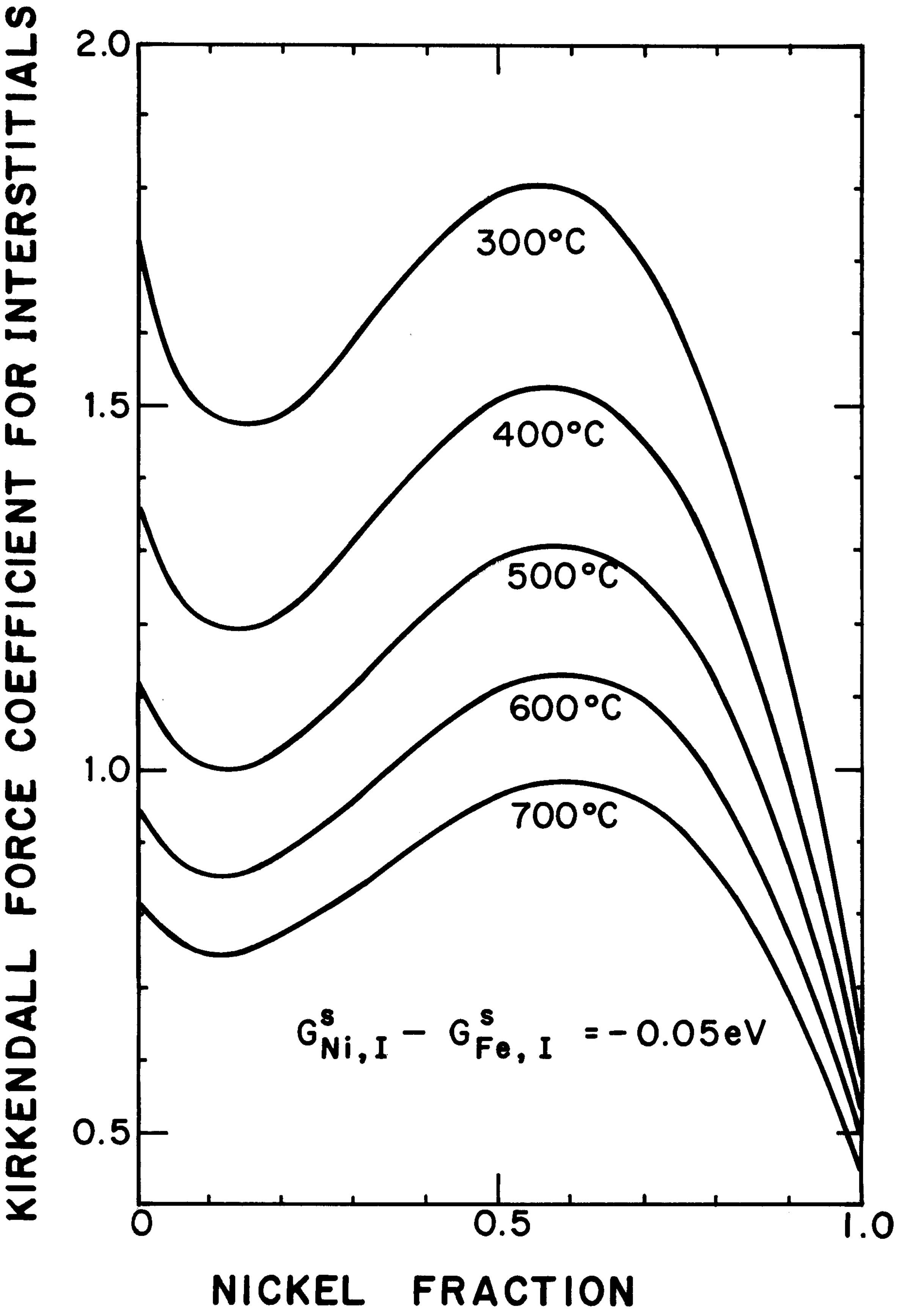

Figure 8 Example of a possible Kirkendall force coefficient for interstitials in binary alloys of iron and nickel.

self-interstitial. However, when it is the slower diffusing species, then K_I is negative and the interstitials are repelled by regions of higher nickel concentration.

Considering the magnitude of the Kirkendall force coefficient K_I, it appears that the Kirkendall force will affect the interstitial bias to a similar degree as it does the vacancy bias. However, the effect could of course be opposite for the two bias factors.

5. CONCLUSIONS

The presence of radiation-induced segregation in an alloy depends on the continuous flux of vacancies and interstitials to sinks and on the unequal mobilities of the alloy constituents. Given these two conditions it then follows by necessity that the compositional gradients will also affect the flux of vacancies and interstitials by introducing additional drift forces. Although the absolute magnitude of each point defect flux will not be changed significantly, the difference between the interstitial and vacancy flux will be altered. In other words, although the average mobility of the point defect is hardly affected by the segregation, the bias can be modified considerably.

The bias modification is basically the result of the following effects. First, the energy of a point defect depends on the local alloy composition. Therefore, when the point defect migrates through a compositional gradient it diffuses either up or down a potential energy gradient. Whether this potential energy increases or decreases depends on three factors: the contribution of interatomic forces to the point defect energy, the dependence of the strain energy of the point defect on the local elastic moduli, and finally, the coherency strain field produced by the non-uniform alloy composition.

These potential energy changes induced by the segregation can be of the same order of magnitude as the mechanical interaction energy of the point defect with the stress field of dislocations, as has been demonstrated here for the case of binary Fe-Ni alloys. It is to be expected that similar changes can also be induced in other alloys where radiation-induced segregation occurs.

In addition to the above potential energy changes, the inverse Kirkendall effect gives rise to an additional drift force. Its effect on the interstitial bias factors appears to be of secondary importance compared to the other effects. However, for vacancy bias factors, the Kirkendall force appears to be significant.

The implications of the present findings are that they may provide a physical basis not only for the understanding of the effect of alloy composition on swelling, but also for alloy development. In principle, radiation-induced segregation has the potential to both increase or decrease the bias. Whether the last possibility can in fact be realized in a particular alloy system will depend on the detailed knowledge of such fundamental properties as elastic moduli, lattice parameter, and tracer diffusion coefficients as a function of alloy composition and temperature. These properties have in the past not been considered essential in the development of radiation-resistant alloys. In view of the new results presented here, however, such properties may contain essential information to assess the radiation damage resistance of an alloy class.

Acknowledgment

This work has been supported by the Division for Basic Energy Sciences, U.S. Department of Energy under contract ER-78-S-02-4861 with the University of Wisconsin.

Appendix A

The energy associated with an elastically strained solid is given by

$$U = \frac{1}{2} \int \sigma_{ij}\varepsilon_{ij} \, dV - \int t_i u_i \, dS - \int f_i u_i \, dV \tag{A1}$$

where

$$\sigma_{ij} = C_{ijk\ell}\varepsilon_{k\ell} = C_{ijk\ell}u_{k,\ell} , \tag{A2}$$

$\vec{u}$ is the displacement vector field, $\vec{t}$ is the load vector on the external surface S, and $\vec{f}$ is the distribution of body forces required to simulate the presence of point defects.

Suppose that the elastic moduli $C_{ijk\ell}(\vec{r})$ are changed to new values $C^0_{ijk\ell}$ while the same body and surface forces are maintained. As shown by Walpole [29] the energy change associated with the modulus change is

$$U - U_0 = \frac{1}{2} \int \varepsilon_{ij}(C_{ijk\ell} - C^0_{ijk\ell})e^0_{k\ell} \, dV \tag{A3}$$

or

$$U - U_0 = \frac{1}{2} \int \sigma_{ij}(S^0_{ijk\ell} - S_{ijk\ell}) \, \sigma^0_{k\ell} \, dV \tag{A4}$$

where $S_{ijk\ell}$ is the compliance tensor and σ^0_{ij} and ε^0_{ij} are the stresses and strains after the modulus change. An upper bound for $(U - U_0)$ can now be obtained when ε_{ij} is replaced by ε^0_{ij} in Eq. (A3), and a lower bound when σ_{ij} is replaced by σ^0_{ij} in Eq. (A4).

For elastically isotropic solids we obtain then

$$\frac{1}{2}\int[(1 - \frac{\mu_0}{\mu})\sigma^0_{ij}\varepsilon^0_{ij} - \frac{1}{3}(\frac{\kappa_0}{\kappa} - \frac{\mu_0}{\mu})\sigma^0_{ii}\varepsilon^0_{jj}]\,dV < U - U_0 < \frac{1}{2}\int[(\frac{\mu}{\mu_0} - 1)\sigma^0_{ij}\varepsilon^0_{ij}$$

$$+ \frac{1}{3}(\frac{\kappa}{\kappa_0} - \frac{\mu}{\mu_0})\sigma^0_{ii}\varepsilon^0_{jj}]\,dV \qquad \text{(A5)}$$

where μ, μ_0 are the shear moduli and κ, κ_0 the bulk moduli.

Let us now assume that μ_0 and κ_0 are constants and that

$$\mu(\vec{r}) = \mu_0 + \delta\mu(\vec{r}) \quad , \quad \kappa(\vec{r}) = \kappa_0 + \delta\kappa(\vec{r}) \ . \qquad \text{(A6)}$$

For small variations, $\delta\mu \ll \mu_0$ and $\delta\kappa \ll \kappa_0$, we can expand the factors containing the elastic moduli. Keeping only linear terms we find that the upper and lower bounds of the inequality (A5) coincide. Therefore, to linear order in $\delta\mu$ and $\delta\kappa$,

$$\delta U = U - U_0 = \frac{1}{2}\int[\frac{\delta\mu}{\mu_0}\,\sigma^0_{ij}\varepsilon^0_{ij} + \frac{1}{3}(\frac{\delta\kappa}{\kappa_0} - \frac{\delta\mu}{\mu_0})\,\sigma^0_{ii}\varepsilon^0_{jj}]\,dV \qquad \text{(A7)}$$

Furthermore, Eq. (A7) still represents an exact upper bound regardless of the magnitude of $\delta\mu$ and $\delta\kappa$.

Suppose now that the stress field σ^0_{ij} is the one produced by a point defect modeled as an inclusion. The inclusion is thought to be formed by expanding a spherical volume Ω to a new volume $\Omega + v$, where v is equal to the relaxation volume of the point defect. Then [19]

$$\sigma^0_{ij}\varepsilon^0_{ij} = \begin{cases} (16\mu_0^2/9\kappa_0)(v/\Omega\gamma)^2 & \text{for } r < r_0 \\ \\ (4\mu_0/3)(v/\Omega\gamma)^2(r_0/r)^6 & \text{for } r > r_0 \end{cases}$$

and

$$\frac{1}{3}\,\sigma^o_{ii}\varepsilon^o_{jj} = \begin{cases} (16\mu_0^2/9\kappa_0)(v/\Omega\gamma)^2 & \text{for } r < r_0 \\ 0 & \text{for } r > r_0 \end{cases}$$

where r_0 is the radius of the sphere with volume Ω and

$$\gamma = (3\kappa_0 + 4\mu_0)/3\kappa_0 \ .$$

It is seen that outside the inclusion, the strain energy density decreases as r^{-6} with increasing distance r from the center of the inclusion. As a result, the dominant contribution to the integral in Eq. (A7) arises from the volume inside and immediately outside the point defect. Therefore, if $\delta\mu$ and $\delta\kappa$ vary little over the volume of the point defect, they may be taken outside the integral and we obtain

$$\delta U = \left\{\frac{3\kappa_0}{3\kappa_0 + 4\mu_0}\,\frac{\delta\mu}{\mu_0} + \frac{4\mu_0}{3\kappa_0 + 4\mu_0}\,\frac{\delta\kappa}{\kappa_0}\right\} \bar{U}^{BR} \qquad (A8)$$

where

$$\bar{U}^{BR} = \frac{1}{2}\int \sigma^o_{ij}\varepsilon^o_{ij}\ dV = \frac{2\kappa_0\mu_0}{3\kappa_0 + 4\mu_0}\,\frac{v^2}{\Omega} \qquad (A9)$$

is the strain energy or bulk relaxation energy of the point defect.

Appendix B

Variations of the lattice parameters introduce an inelastic strain distribution of $e_{ij} = \delta_{ij}\eta(\vec{r})$ into the solid similar to thermal strains. The associated stress distribution can be obtained from the equilibrium conditions $\sigma_{ij,j} = 0$, where an index preceded by a comma indicates partial differentiation. Using Hooke's law

$$\sigma_{ij} = \mu(u_{i,j} + u_{j,i} - 2e_{ij}) + \frac{2\mu\nu}{1 - 2\nu}\delta_{ij}(u_{\kappa,\kappa} - e_{\kappa\kappa}) \qquad \text{(B1)}$$

one obtains

$$u_{i,jj} + \frac{1}{1 - 2\nu} u_{j,ji} = 2\frac{1 + \nu}{1 - 2\nu} \eta_{,i} \; . \qquad \text{(B2)}$$

If we write $\vec{u} = \vec{\nabla}\phi$, then Eq. (B2) yields

$$\nabla^2\phi = \frac{1 + \nu}{1 - \nu}\eta \; . \qquad \text{(B3)}$$

The elastic dilatation is now given by

$$\varepsilon_{ii} = u_{i,i} - 3\eta = \nabla^2\phi - 3\eta = -2\frac{1 - 2\nu}{1 - \nu}\eta \; . \qquad \text{(B4)}$$

The size interaction of a point defect with this elastic strain field yields then the coherency strain interaction

$$U^C = -v\kappa\varepsilon_{ii} = 2v\kappa\frac{1 - 2\nu}{1 - \nu}\eta(\vec{r}) \; . \qquad \text{(B5)}$$

Using the expression for the bulk relaxation energy $\overline{U}^{BR}$ we find

$$U^{C} = \mu \frac{\Omega}{V} \overline{U}^{BR} \eta(\vec{r}) \ . \tag{B6}$$

References

[1] Workshop on Solute Segregation and Phase Stability During Irradiation; ed. by J.O. Stiegler, J. Nucl. Materials 83 (1979) 1-237.

[2] Phase Stability During Irradiation; ed. by J.R. Holland, L.K. Mansur, and D.I. Potter, The Metallurgical Soc. of AIME, 1981.

[3] W.G. Wolfer and L.K. Mansur, J. Nucl. Materials 91 (1980) 265.

[4] A. Si-Ahmed and W.G. Wolfer, ASTM STP 782 (1982) 1008.

[5] F.A. Garner, Ref. 2, p. 165.

[6] W.G. Johnston, W.G. Morris, and A.M. Turkalo, in "Rad. Effects in Breeder Reactor Structural Materials," eds. M.L. Bleiberg and G.W. Bennet, Met. Soc. AIME, New York, 1977, p. 421.

[7] H.R. Brager and F.A. Garner, J. Nucl. Materials 73 (1978) 9.

[8] D.L. Porter, J. Nucl. Materials 79 (1979) 406.

[9] D.L. Porter and E.L. Wood, J. Nucl. Materials 83 (1979) 90.

[10] H.R. Brager and F.A. Garner, ASTM STP 683 (1979) 207; ASTM STP 725 (1981) 470.

[11] W.J.S. Yang, H.R. Brager, and F. Garner, Ref. [2], p. 257.

[12] A.D. Marwick, J. Phys. F.: Metal Phys. 8 (1978) 1849.

[13] R. Cauvin, Doctoral Thesis, L'Université Nancy I, August 1981, also: Rapport CAE-R-5105.

[14] R. Cauvin and G. Martin, Phys. Rev. B23 (1981) 3333.

[15] J.R. Manning, "Diffusion Kinetics for Atoms in Crystals," D. van Nostrand, Princeton, 1968, Ch. 6.

[16] Y. Adda and J. Philibert, "La Diffusion dans les Solides," Presses Universitaires de France, 1966, p. 596.

[17] H. Wiedersich, P.R. Okamoto, and N.Q. Lam, J. Nucl. Materials 83 (1979) 98.

[18] W.G. Wolfer and L.K. Mansur, Phys. Stat. Sol.(a) 37 (1976) 211.

[19] J.D. Eshelby, Solid State Phys. 3 (1956) 79.

[20] W.G. Wolfer and M. Ashkin, J. Appl. Phys. 47 (1976) 791.

[21] W.G. Wolfer and M. Ashkin, J. Appl. Phys. 46 (1975) 547.

[22] A.D. Marwick, W.A.D. Kennedy, D.J. Mazey, and J.A. Hudson, Scripta Met. 12 (1978) 1015.

[23] H.R. Brager and F.A. Garner, TMS-AIME Symp. Adv. Techniques for Characterization of Irrad. Metals, Las Vegas, Feb. 1980, in press.

[24] L.E. Thomas, to be published in Ultramicroscopy.

[25] G. Hausch and H. Warlimont, Acta Met. 21 (1973) 401; Z. Metallkunde 63 (1972) 547.

[26] E.A. Owen and E.L. Yates, Proc. Phys. Soc. 49 (1937) 17, 178, 307.

[27] B. Million, J. Rozickova, J. Velisek, and J. Vrestal, Mater. Sci. Eng. 50 (1981) 43.

[28] Y. Tanji, Y. Nakagawa, Y. Saito, K. Nishimura, and K. Nakatsuka, Phys. Stat. Sol.(a) 56 (1979) 513.

[29] L.J. Walpole, J. Mech. Phys. Solids 18 (1970) 343.